Microelectronic Engineering 128 (2014) 12–18

Contents lists available at ScienceDirect

Microelectronic Engineering

journal homepage: www.elsevier.com/locate/mee

Fabrication and characterization of gold coated hollow silicon microneedle array for drug delivery

K.B. Vinayakumar [a], G.M. Hegde [b], M.M. Nayak [b], N.S Dinesh [c], K. Rajanna [a,*]

[a] Department of Instrumentation and Applied Physics, Indian Institute of Science, Bangalore 5600012, India
[b] Centre for Nano Science and Engineering, Indian Institute of Science, Bangalore 5600012, India
[c] Department of Electronic Systems Engineering, Indian Institute of Science, Bangalore 5600012, India

ARTICLE INFO

Article history:
Received 8 April 2014
Received in revised form 12 May 2014
Accepted 31 May 2014
Available online 10 June 2014

Keywords:
Microneedles
Dry etching
Sputtering
Electroplating

ABSTRACT

In this paper, we present the fabrication and characterization of Ti and Au coated hollow silicon microneedles for transdermal drug delivery applications. The hollow silicon microneedles are fabricated using isotropic etching followed by anisotropic etching to obtain a tapered tip. Silicon microneedle of 300 μm in height, with 130 μm outer diameter and 110 μm inner diameter at the tip followed by 80 μm inner diameter and 160 μm outer diameter at the base have been fabricated. In order to improve the biocompatibility of microneedles, the fabricated microneedles were coated with Ti (500 nm) by sputtering technique followed by gold coating using electroplating. A breaking force of 225 N was obtained for the fabricated microneedles, which is 10 times higher than the skin resistive force. Hence, fabricated microneedles can easily be inserted inside the skin without breakage. The fluid flow through the microneedles was studied for different inlet pressures. A minimum inlet pressure of 0.66 kPa was required to achieve a flow rate of 50 μl in 2 s with de-ionized water as a fluid medium.

1. Introduction

Oral drug administration is commonly employed by the physicians for treating diseases like diabetes, etc. However, oral drug administration is not always feasible due to poor drug absorption through gastrointestinal tract. Transdermal drug delivery technology has emerged as the most common approach to overcome this disadvantage [1,2]. Furthermore, transdermal drug delivery technology has many advantages such as, a specific skin area can be targeted. Also, dose reduction and precise control over volume of drug can be achieved. In addition, use of microneedles in transdermal drug delivery system causes less pain which helps in treating patients having needle phobia.

Out of plane microneedles have tremendous applications in drug delivery system and body fluid extraction [3]. Geometrical constraints on these microneedles are imposed by the physiology of human skin. Fig. 1 shows the cross section of human skin together with microneedles array. The outer most layer of the human skin is known as stratum corneum (20–30 μm thick). The next layer is epidermis with a thickness of 100 μm [4,5]. For painless epidermal drug delivery, it is desirable that the microneedle has to penetrate to a depth of 150–200 μm within the skin. These requirements impose constraint on the length of the microneedle to be in the range of 150–200 μm. Previously, in order to reduce the insertion force and hence to avoid the possible needle damage while inserting into the tissues, as well as the possible needle blockage, different shapes of silicon (Si) microneedles have been reported in the literature. Table 1 gives an overview of the reported typical dimensions of the hollow Si microneedles fabricated till date. Griss et al. and Gardenier et al. have demonstrated the sharp tip microneedles with side openings. However, the disadvantage with the side opened microneedle is, opening is too far from the needle tip. Thus, the needles need to be inserted much deeper into the tissue to avoid drug leakage. Khanna et al. reported the microneedle having opening in the tip. But, in their approach the tapering of microneedles tip was achieved by gradual reduction of the photoresist method, which involves multiple steps [6].

One of the most important requirements for microneedles is the material biocompatibility with skin and the drugs. Technologies have been established to realize biocompatible microneedles using various materials including metals and polymers [7]. However, Si is not well established as a biocompatible material for implantable bio-devices unlike well studied materials like titanium, stainless steel and gold [8]. Processing of polymer, metal and stainless steel for micro fabrication still needs extensive research for mass production. Hence we have explored the possibility of taking advantage of well established Si technology for fabricating microneedle

* Corresponding author. Tel.: +91 80 22933188; fax: +91 80 23600135.
E-mail addresses: kraj@isu.iisc.ernet.in, krajanna2003@yahoo.com (K. Rajanna).

http://dx.doi.org/10.1016/j.mee.2014.05.039
0167-9317/

Table 1
Typical properties of the hollow out-of plane Si microneedles.

Reference typical dimensions (μm)	Khanna et al. [6]	Griss et al. [19]	Gardenier et al. [9]	Stoeber et al. [4]	Ashraf et al. [10]	Jurcícek et al. [11]
Inner diameter	118.8	60	70	40	60	10–25
Outer diameter (tip)	119.8	10	0	50	–	–
Outer diameter (base)	165	160	250	425	150	–
Length	200	250	350	200	250	100–120

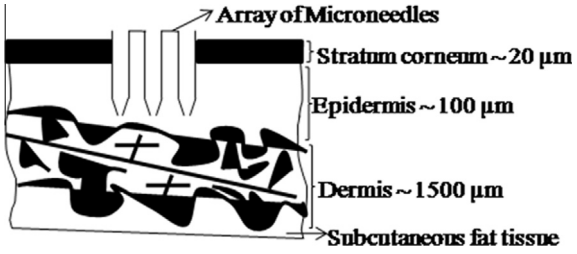

Fig. 1. Cross-section of human skin.

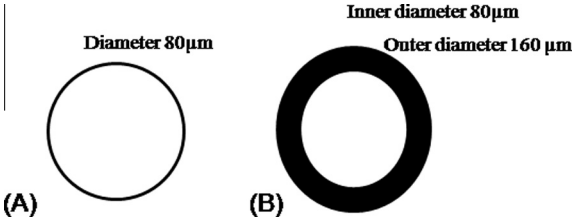

Fig. 2. Mask design for hollow Si microneedles. (A) Back side mask for inner lumen. (B) Front side mask for inner lumen and needle walls.

with minimum process steps and coating them with biocompatible material to make it a cost effective biocompatible device for drug delivery.

In this paper, we present the design and fabrication of tapered hollow out of plane Si microneedle by single step isotropic and anisotropic process using Deep Reactive Ion Etching (DRIE). The fabricated microneedles were coated with titanium (Ti) by sputtering and gold (Au) by electroplating method to make it suitable for implantable bio-devices. The mechanical failure of the microneedles was experimented using suitable in-house built experimental setup. Fluid flow through the array of microneedles was studied for different inlet pressures.

2. Experimental

2.1. Fabrication of flat tip microneedles

In this work, we have employed two-step lithography process for the realization of microneedles. Fig.2 shows the mask structures used to fabricate microneedles and Fig. 3 shows the graphical illustration of steps involved for fabrication. Initially, a double side polished four inch Si wafer was cleaned in piranha solution for 15 min. The cleaned wafer was oxidized using thermal oxidation furnace (dry-wet-dry oxidation) and this creates a SiO_2 layer (about 1 μm) on both sides of Si wafer. The SiO_2 thickness is confirmed by ellipsometer (step1 in Fig. 3). Photolithography was carried out from backside to etch the inner bore of Si wafer using a mask structure shown in Fig. 2A. The patterned SiO_2 on the backside of the Si wafer is etched by Reactive Ion Etching (RIE) as shown in step 2 of Fig. 3. This process is followed by DRIE to etch Si from backside for a depth of 160 μm and is shown in step 3 of Fig. 3 (using Bosch process, 15 μm min^{-1} is employed). In the next step, photolithography was carried out from front side of the wafer to etch Si using a mask structure shown in Fig. 2B. The patterned SiO_2 on the front side of the Si wafer is etched by RIE is shown in step 4 of Fig. 3. The mask is designed to etch both hole and pillar structures using a single mask as shown in step 5 of Fig. 3. Therefore, SiO_2 is left only on top of the microneedle wall region. Using RIE process, the SiO_2 on top of the microneedle wall is removed to get Si microneedles. Finally, an array of hollow Si microneedles having a height 300 μm was obtained with 80 μm inner and 160 μm outer diameters as shown in Fig. 4.

2.2. Fabrication of tapered tip microneedles

Si microneedles fabricated using the above mentioned process does not have tapered tip to facilitate easy penetration into the skin. It is a known fact that, microneedles without tapered end require more force to penetrate into the skin [6]. Therefore, we have fabricated microneedles with tapered tip using isotropic etching process (15 μm/min undercut and 15 μm/min deep etch recipe is used). Subsequent to step 4 indicated in Fig. 3, one minute isotropic etching (as shown in step A of Fig. 5) has been carried out which is followed by anisotropic etching to achieve a tapered tip with top oxide layer (as shown in step B of Fig. 5). In order to obtain tapered tip, the top oxide on the microneedles is removed using RIE process which is schematically shown in step C of Fig. 5. Fig. 6B shows the fabricated tapered tip microneedle with oxide layer on the top. The top oxide layer on the microneedle tip was removed using RIE process (shown in step A of Fig. 4). Finally, an array of hollow tapered Si microneedles of height 300 μm was obtained with 130 μm outer diameter and 110 μm inner diameters at the tip.

2.3. Metal coating on microneedles

Further, Si microneedles are coated with Ti and Au to make them suitable for implantable bio-device. A seed layer of Ti metal of thickness 500 nm was coated on Si microneedles using sputtering method as shown in Fig. 7. The conductive seed layer is necessary for electroplating of Au. Therefore, 1 μm thick Au was deposited on the Ti coated Si microneedles. After coating Ti and Au on microneedles, the through hole of the microneedle was confirmed by using an optical microscope (with the illuminating light) as shown in the Fig. 8. Microneedle insertion and liquid flow was studied by connecting microneedle substrate to a 6 mm silicone tube using PolyDiMethylSiloxane (PDMS) as shown in Fig. 9. Ti deposition on inside as well as outside of the needle wall was examined by making a vertical cross sectional cut (shown in Fig. 10A) using Focused Ion Beam (FIB) technique. The presence of Ti layer confirmed using Energy Dispersive X-ray technique (EDAX) is shown in Fig. 10.

2.4. Mechanical strength and adhesion

An experiment was carried out in order to estimate the breaking force of the microneedles. The schematic of the experimental setup used is shown in Fig. 11. It essentially consists of a solid aluminum rod, microneedle array, aluminum supporting plates and a load cell. In order to measure the breaking force for microneedles, the axial load is applied on the microneedles using a load cell. The load cell is made to move slowly towards the microneedle array at a speed of 2.5 μm ms^{-1}, and the measured microneedle breaking

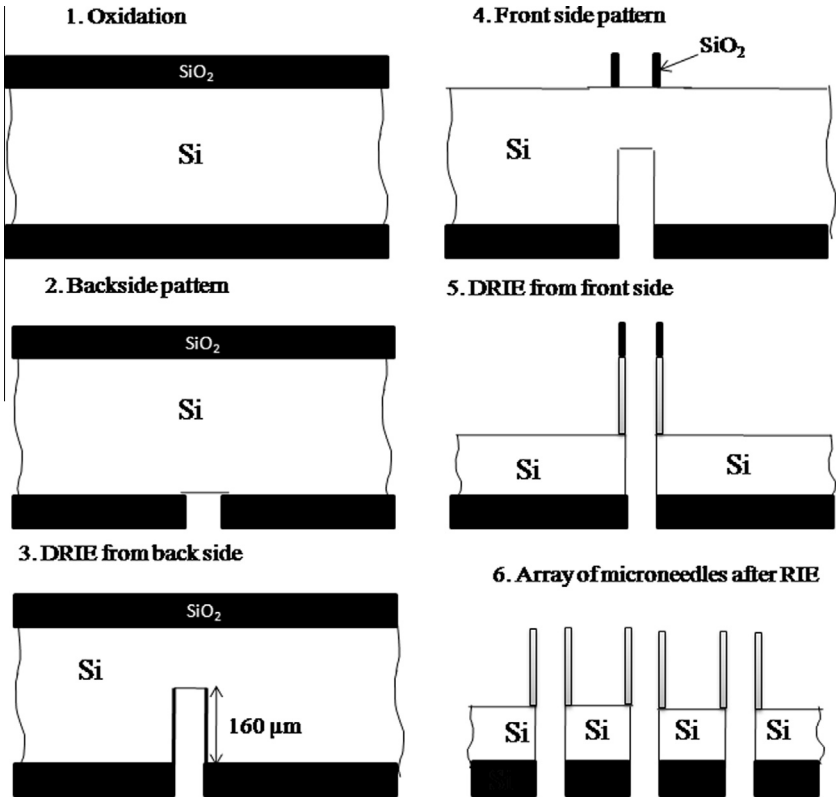

Fig. 3. Process flow for the fabrication of out-of-plane hollow Si microneedles.

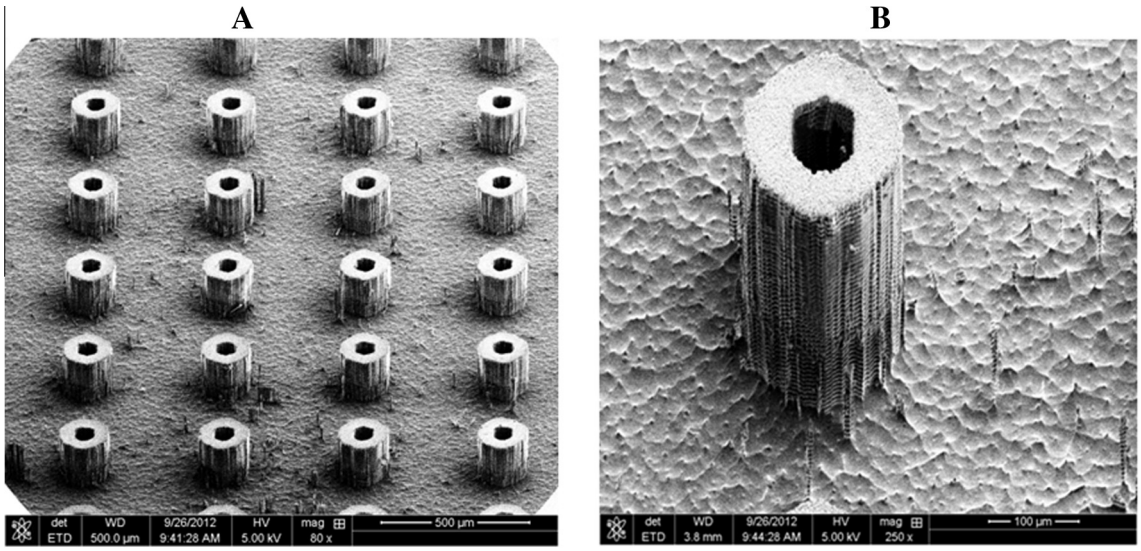

Fig. 4. SEM image of hollow Si microneedles, the length of the structure is 210 µm. (A) An array of microneedles, the separation between needles in the array is 500 µm. (B) Single flat tip microneedle.

force was recorded. Fig. 12 shows the variation of critical breaking force versus displacement.

2.5. Fluid flow characterization through the microneedles

The fluid flow characteristics through the microneedles are studied using a setup shown in Fig. 13. An array of microneedle patch is connected with a silicone tube (6 mm inner diameter) through 3 way valve to provide an inlet to the pressure sensor port. Extended tube from 3-way valve is connected to sphygmomanometer to control the pressure by changing the mercury level in it. Pressure is increased in steps of 0.65 kPa and the liquid from microneedles patch is collected separately at different pressures. After each minute, the quantity of liquid collected is measured and the flow rate versus pressure plot was generated (Fig. 14).

3. Results and discussion

A 10×10 array of Si microneedles with flat tip having inner diameter and outer diameter 80 and 160 µm respectively is shown in Fig. 4. It is possible to vary the inner diameter and outer diameter of the microneedle, depending on the skin hardness, flow rate

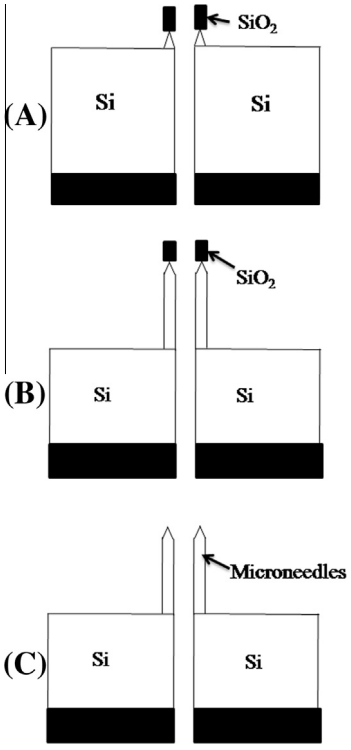

Fig. 5. Process flow for the fabrication of tapered tip Si microneedles. (A) Isotropic etching of Si. (B) Anisotropic etching followed by isotropic etching. (C) Tapered microneedles after removing top oxide.

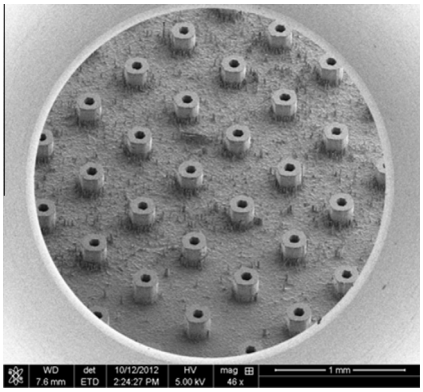

Fig. 7. SEM image of the Ti coated Si microneedles.

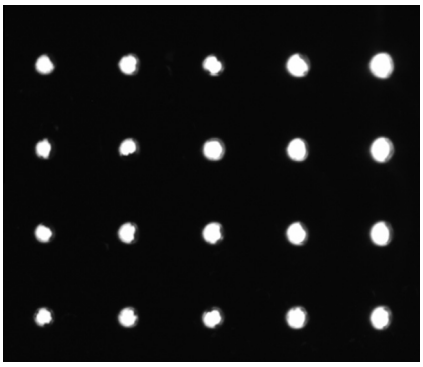

Fig. 8. Light illumination test through the microneedle hole, performed using optical microscope.

and the material of the microneedle. Keeping this in mind and the convenience of fabrication process facility available with us, we have fabricated microneedles of inner diameter and outer diameter 80 and 160 μm respectively.

Since flat tip microneedles need more insertion force compared to tapered tip microneedles [6], the tapered tip microneedles are of interest due to their easy insertion into skin. In our study, we have achieved the tapering of microneedle by isotropic etching process. The tapered microneedle image is as shown in Fig. 6A. It shows that the microneedle fabrication started with isotropic etching followed by anisotropic etching. The isotropic etching is used to obtain tapered tip microneedle by taking the advantage of undercut and anisotropic etching was carried out to obtain the desired height. Fig. 6B shows the microneedle tip covered with top oxide layer and the undercut region. After removing the top oxide by RIE, the tapered microneedles were obtained and are shown in Fig. 6C. After isotropic etching, the tip diameter of the microneedle is reduced to 130 μm. It is still possible to get sharper tip microneedles by increasing the isotropic etching time. However, for this purpose, the SiO_2 layer quality should be extremely good. In our case, the oxide layer was falling down after increasing the isotropic etching time beyond 1 min duration. Therefore, we stopped the isotropic etching after 1 min and continued with anisotropic etching to obtain the desired height using the same SiO_2 oxide mask as shown in Fig. 6B.

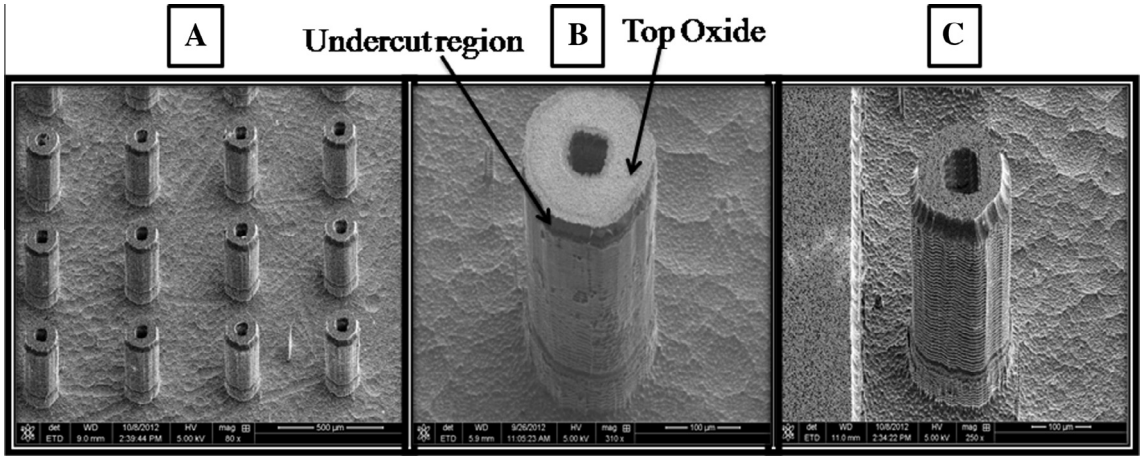

Fig. 6. SEM image of tapered hollow Si microneedles, the length of the structure is 300 μm. (A) An array of tapered microneedles. The separation between needles in the array is 500 μm. (B) A single tapered microneedle with top oxide. (C) After removing oxide layer, left with tapered microneedle.

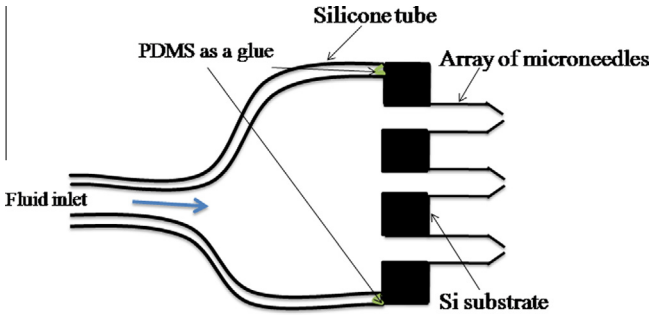

Fig. 9. Schematic of array of microneedles connected to silicone tube using PDMS to perform liquid flow characterization.

It may be noted that, Si is not a well studied material for implantable bio-devices [8] unlike SiO_2 coated Si microneedles [12] and metal microneedles [13,14]. Fabricating the array of metal and stainless steel microneedles is not feasible by using conventional micromachining techniques compared to micromachining of Si. Hence in our study, we have deposited Ti and Au on the fabricated Si microneedles to make Si microneedles more suitable for implantable bio-devices. A 500 nm thick Ti was deposited on Si microneedles by sputtering technique (Fig. 7). It can be seen that the microneedle outer wall and the tips are completely coated with Ti, which acts as a seed layer to deposit Au [13]. After depositing Ti and Au, the through hole of the microneedle was confirmed by using an optical microscope (with light illumination) as shown in Fig. 8. This enabled us to confirm that all the holes in microneedle substrate are open, which is not possible just by liquid flow characterization. Along with the outer wall, the inner wall of the microneedle were also coated with Ti but the thickness is not same at all the places. This discrepancy is due to the limited opening and the line of sight effect, which is a common problem with sputtering technique. Thickness of the Ti is higher near the tip of the microneedle and it slowly reduces with depth. This fact was confirmed by EDAX analysis after making a narrow vertical cut (as shown in Fig. 10) using FIB technique. Ti is not very stable as it oxidizes easily when it is exposed to external environment. Therefore, 1 μm thick Au was coated on Ti coated microneedles by electroplating to avoid the oxidation of Ti. While inserting these needles into the skin, skin makes contact only with Au and not with Si. Hence, coated Si microneedles can be used for implantable bio-devices.

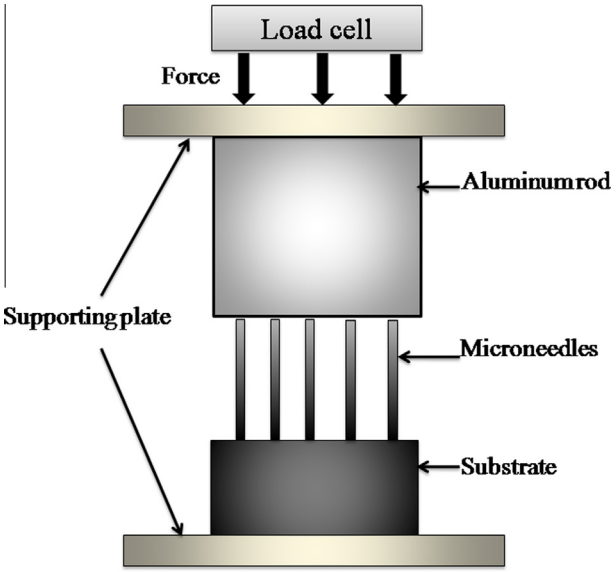

Fig. 11. Schematic of microneedle failure mechanism analysis.

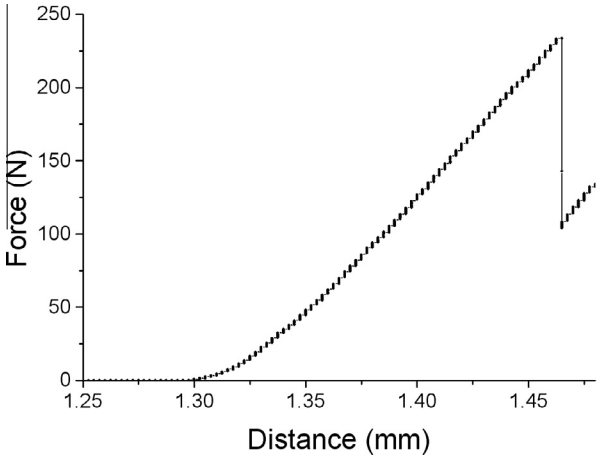

Fig. 12. Measured load–displacement curve for the microneedle.

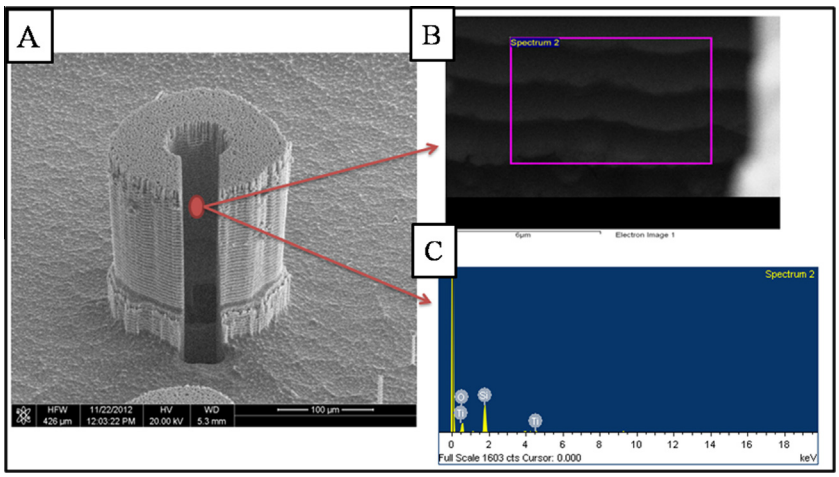

Fig. 10. (A) Cross section of microneedle prepared using FIB. (B) Expanded view of the microneedle to take EDAX. (C) EDAX spectrum taken from the expanded area.

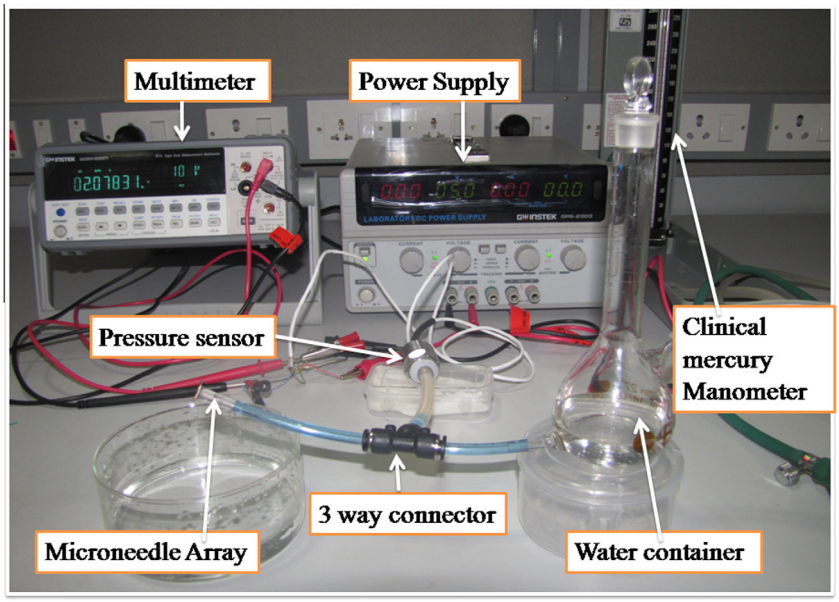

Fig. 13. Experimental setup used for fluid flow characterization of array of microneedles.

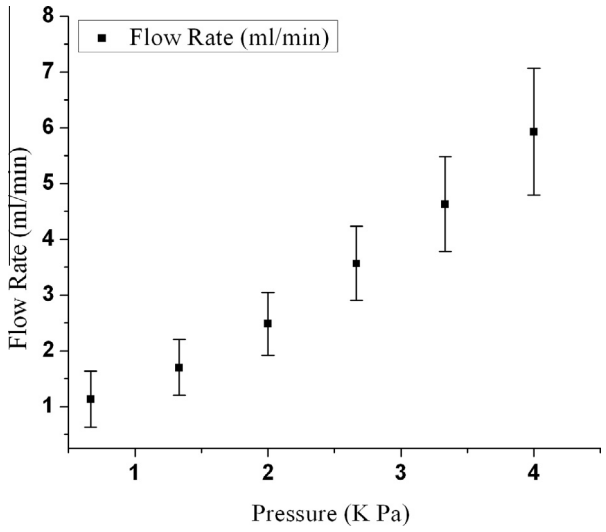

Fig. 14. Variation of fluid flow rate versus inlet pressure through microneedle.

The variation of load versus displacement curve for an array of microneedles is shown in Fig. 12. The load was applied onto the microneedles until they breaks, indicating the ultimate load that they can withstand. This was indicated by the discontinuity in the applied force versus displacement curve (Fig. 12). This was also confirmed by visual observation. Once the microneedles break, the load continues to drop significantly far below the ultimate load. Human skin is known to offer a resistive pressure of 3.18 MPa [15]. In our experiment, we have observed that, the ultimate pressure at which an array of microneedles break is ~38 MPa, which is much above the skin resistive pressure. Khanna et al. and Yan et al. reported that the insertion force of the microneedle decreases by reducing the tip area [8,16]. In addition, few studies have shown that there is a possibility of breaking of sharp tip microneedles during insertion [17,18]. While designing the microneedles, the separation between microneedles is also important to avoid bed-of-nails effect. To check the bed-of-nail effect, the fabricated microneedles were successfully inserted and removed from the medium hard silicone rubber and observed the microneedles impression on the silicone rubber. This mark showed that the fabricated array of microneedles with 500 μm pitch is good enough for insertion to avoid bed-of-nail effect. The Ti and Au adhesion on Si microneedles was found to be excellent to insert into silicone rubber. This result shows that the designed microneedle is strong enough to penetrate into the human skin without breaking.

The study of drug flow through the skin using microneedles is a field of extensive research [4]. The motion of fluid in the skin is not continuous due to the presence of tissues, so that highly nonlinear effects are expected [18,19]. Therefore, the present flow characterization is restricted to fluid flow ejection into open air using water as a fluid medium [2]. Liquid flow through the microneedle was studied using a specially made experimental setup shown in Fig. 13. In the present study, we discuss the liquid flow through the microneedle using water as a fluid medium [4]. Due to surface tension, the separation between the microneedles is not adequate enough to study the liquid flow through single microneedle. Therefore, the water molecules from each microneedle will combine and form a single water droplet to reduce its surface energy which was observed through an experiment. Typical transdermal drug delivery (Insulin) demands a delivery of 50–100 μl in 2 s [19]. Griss et al. achieved 100 μl volume of aqueous fluid through 21 microneedles in 2 s with a pressure drop of 2 kPa [19,20]. Moreover, they proposed that the flow resistance could be further reduced by increasing the number of microneedles. In our present study, we achieved a pressure drop of 0.66 kPa for a flow of 50 μl in 2 s using 100 microneedles. The quantity of liquid coming out from microneedle array can be increased by increasing the inlet pressure. We observed that, after some threshold (after 3.99 kPa) the liquid begins to form jet instead of drops. By increasing the inlet pressure, the quantity of liquid flow will increase and controlling of liquid flow rate will be difficult. Hence, we restricted our study in the pressure range from 0.66 to 3.9 kPa (bubble forming range) which is sufficient to deliver drug in a controlled manner. Variation of flow rate of water with respect to inlet pressure is shown in Fig. 14. This clearly shows that a controlled drug delivery can be achieved by controlling the inlet pressure, thereby allowing a known quantity of the drug to be injected into the body. Thus we have proposed a simple and cost effective process for the real-

ization of biocompatible microneedles array suitable for transdermal drug delivery.

4. Conclusion

We have described a simple and cost effective process for fabricating tapered tip Si microneedles using isotropic and anisotropic etching processes. The outer wall region of the Si microneedle is coated with Ti/Au layers to improve its biocompatibility. We have characterized the fabricated microneedles for their mechanical stability and flow rate at different in-let pressures. The measured breaking force of the fabricated microneedles is much higher than the skin resistive force, which indicates the easy insertion of microneedles into the skin without the possibility of fracture. Fluid flow through the array of microneedles has been studied for different in-let pressures. It is observed that a minimum inlet pressure of 0.66 kPa was required to achieve a minimum flow rate of 50 μl in 2 s. Performance study carried out on Au coated Si microneedles indicated the possible replacement of these with metal microneedles for implantable bio-devices.

Acknowledgments

The authors gratefully acknowledge the financial support from NPMASS, India, and also thank CeNSE, IISc for the facilities. We also acknowledge the kind help from Mr. Ranjith in sputtering, Mr. Vamsi K.N. for his help in fabricating the microneedles, Ms. Suma B.N. and Mr. Vardharaju for SEM imaging and FIB, and Mr. Pandian for his help in liquid flow characterization.

References

[1] A. Arora, M.R. Prausnitz, S. Mitragotri, Int. J. Pharm. 364 (2008) 227.
[2] M. Matteucci, M. Casella, M. Bedoni, E. Donetti, M. Fanetti, F.D. Angelis, F. Gramatica, E.D. Fabrizio, Microelectron. Eng. 85 (2008) 1066.
[3] N. Roxhed, T.C. Gasser, P. Griss, G.A. Holzapfel, G. Stemme, J. Microelectromech. Syst. 16 (6) (2007) 1429.
[4] B. Stoeber, D. Liepmann, J. Microelectromech. Syst. 14 (2005) 472.
[5] N. Roxhed, B. Samel, L. Nordquist, P. Griss, G. Stemme, IEEE Trans. Biomed. Eng. 55 (2008) 1063.
[6] P. Khanna, K. Luongo, J.A. Strom, S. Bhansali, J. Micromech. Microeng. 20 (2010) 045011.
[7] D.V. McAllister, P.M. Wang, S.P. Davis, J.-H. Park, P.J. Canatella, M.G. Allen, M.R. Prausnitz, Proc. Natl. Acad. Sci. 100 (2003) 13755.
[8] G. Voskerician, M.S. Shive, R.S. Shawgo, H.v. Recum, J.M. Anderson, M.J. Cima, Robert Langer, Biomaterials 24 (2003) 1959.
[9] H.J.G.E. Gardeniers, R. Luttge, E.J.W. Berenschot, M.J.D. Boer, S.Y. Yeshurun, M. Hefetz, R.v. Oever, A.v.d. Berg, J. Microelectromech. Syst. 12 (2003) 855.
[10] M.W. Ashraf, S. Tayyaba, A. Nisar, N. Afzulpurkar, D.W. Bodhale, T. Lomas, A. Poyai, A. Tuantranont, Cardiovasc. Eng. 10 (2010) 91.
[11] P. Jurčíček, H. Zou, S. Zhang, C. Liu, Nano Lett. 8 (2013) 78.
[12] S. Kim, S. Shetty, D. Price, and S. Bhansali. In: Engineering in Medicine and Biology Society, 2006. EMBS'06. 28th Annual International Conference of the IEEE, IEEE, (2006) 4088.
[13] S.P. Davis, W. Martanto, M.G. Allen, M.R. Prausnitz, IEEE Trans. Biomed. Eng. 52 (2005) 909.
[14] D.G. Koutsonanos, E.V. Vassilieva, A. Stavropoulou, V.G. Zarnitsyn, E.S. Esser, M.T. Taherbhai, M.R. Prausnitz, R.W. Compans, I. Skountzou, Sci. Rep. (2012) 2–4.
[15] P. Aggarwal, C.R. Johnston, Sens. Actuators B 102 (2004) 226.
[16] X.-X. Yan, J.-Q. Liu, S.-D. Jiang, B. Yang, C.-S. Yang, Microelectron. Eng. 111 (2013) 33.
[17] S.P. Davis, B.J. Landis, Z.H. Adams, M.G. Allen, M.R. Prausnitz, J. Biomech. 37 (2004) 1155.
[18] N. Wilke, A. Mulcahy, S.-R. Ye, A. Morrissey, Microelectron. J. 36 (2005) 650.
[19] P. Griss, G. Stemme, J. Microelectromech. Syst. 12 (2003) 296–301.
[20] R.K. Sivamani, B. Stoeber, G.C. Wu, H. Zhai, D. Liepmann, H. Maibach, Skin Res. Technol. 11 (2005) 152.